An Investigation Into Time Domain Features of Surface Electromyography to Estimate the Elbow Joint Angle

TRIWIYANTO[1,3], Oyas WAHYUNGGORO[1], Hanung Adi NUGROHO[1], HERIANTO[2]

[1]Department of Electrical Engineering & Information Technology, Faculty of Engineering, Universitas Gadjah Mada, Jl. Grafika 2, 55281 Yogyakarta, Indonesia
[2]Department of Mechanical & Industrial Engineering, Faculty of Engineering, Universitas Gadjah Mada, Jl. Grafika 2, 55281 Yogyakarta, Indonesia
[3]Department of Electromedical Engineering, Politeknik Kesehatan Surabaya, Ministry of Health Indonesia Pucang Jajar Timur 10, 60282 Surabaya, Indonesia

triwiyanto123@gmail.com, oyas@ugm.ac.id, adinugroho@ugm.ac.id, herianto@ugm.ac.id

DOI: 10.15598/aeee.v15i3.2177

Abstract. *In literature, it is well established that feature extraction and pattern classification algorithms play essential roles in accurate estimation of the elbow joint angle. The problem with these algorithms, however, is that they require a learning stage to recognize the pattern as well as capture the variability associated with every subject when estimating the elbow joint angle. As EMG signals can be used to represent motion, we developed a non-pattern recognition method to estimate the elbow joint angle based on twelve time-domain features extracted from EMG signals recorded from bicep muscles alone. The extracted features were smoothed using a second order Butterworth low pass filter to produce the estimation. The accuracy of the estimated angles was evaluated by using the Pearson's Correlation Coefficient (PCC) and Root Mean Square Error (RMSE).The regression parameters (Euclidean distance, R^2 and slope) were then calculated to observe the effect of the features on elbow joint angle estimation. In this investigation, we found that for a 10-second long recording period, the MyoPulse Percentage (MYOP) Rate produced the best accuracy: with PCC of* 0.97 ± 0.02 *(Mean±SD) and RMSE of* $11.37 \pm 3.04°$ *(Mean±SD), respectively. The MYOP feature also showed the highest R^2 and slope value of* 0.986 ± 0.0083 *(Mean's) and* 0.746 ± 0.17 *(Mean's), respectively for flexion and extension motions during all recorded periods.*

Keywords

EMG, feature extraction, non-pattern recognition, time domain features.

1. Introduction

Surface ElectroMyoGraphy (EMG) is often used to control an assist device such as the upper and lower limb exoskeletons with the function to support human life [1]. It is obvious that the EMG signal can be related to the human limb motion. Several efforts on EMG signal detection have been made to investigate the relationships between muscle groups and limb movement [2] and [3]. In the EMG detection stage, Tang et al. [4] collected EMG signal from four muscle groups located at biceps brachii, brachioradialis, triceps, and anconeus to estimate the elbow joint angle. Benitez et al. [5] recorded the EMG signals from two muscle groups located at biceps and triceps to develop an orthotic system. The methods that utilize more muscle groups in estimating the elbow joint angle, however, would require more computational complexities in data processing.

In order to get information related to elbow joint motion, the recorded EMG signal should be processed by using time, frequency, or time-frequency domain methods to produce informative features. After the feature extraction stage, the EMG features can represent useful information related to the joint angle, force, and torque. Choosing an appropriate feature is essential because it determines the accuracy of the estimation. Some previous studies have preferred to use time domain features over those extracted from frequency and time-frequency domains to predict joint angle [6] and [7] and torque [8]. This preference is due to reduced complexity in data processing and the application of a simple algorithm to be implemented in the real time control. Generally, after the feature extraction process, the joint angle or torque is estimated using a machine learning algorithm or a classifier to improve the accuracy. The methods used in human-machine interaction based on EMG control, are divided into two categories: pattern recognition and non-pattern recognition [1] methods. In the pattern recognition methods, some previous studies used artificial neural networks [4], fuzzy controllers [1], and support vector machines [10] as their classifiers. The limitation in the pattern recognition methods, however, is that the system needs to be trained for each different subject due to the variability in the EMG signal. Therefore, in some cases, this method is not practically applicable. In the non-pattern recognition methods, some previous studies used onset analysis, proportional control, and threshold control [11] and [12]. These methods are simple to be implemented but their accuracies tend to be low. There is also limited literature on elbow-joint angle estimation using non-pattern recognition methods.

Although some efforts have been dedicated to pattern recognition and non-pattern recognition methods for elbow-joint angle estimation, there are still some limitations that should be addressed in furthering this research. Therefore, the purpose of this study is to develop a non-pattern recognition method for estimating the elbow joint angle using a single muscle group (biceps). To implement the proposed method, twelve time-domain features were investigated and a second-order Butterworth low pass filter was applied to filter the features. The specific objectives of the study are to:

- evaluate the accuracy of EMG features in estimating the elbow joint angle using the Pearson's Correlation Coefficient (PCC) and the Root Mean Square Error (RMSE),
- evaluate the regression parameters (Euclidean distance, R-squared, and slope) that relate to the elbow joint angle.

2. Theoretical Background

2.1. Time Domain Features

The recorded EMG signal was extracted to get the features that related to the human elbow-joint angle during flexion and extension motions. In this study, twelve Time-Domain (TD) features were extracted to estimate the elbow joint angle. These features were classified into three categories (based on energy, complexities, and frequency information) [13]. The energy-based features were as follows: the Root Mean Square (RMS), Integrated EMG (IEMG), Variance (VAR), and Mean Absolute Value (MAV). The complexity of the EMG signal could be quantified by using the Waveform Length (WL), Average Amplitude Change (AAC), and Difference Absolute Standard Deviation Value (DASDV) features. The calculated frequency-based informative features were as follows: Zero Crossing (ZC), Sign Slope Change (SSC), Wilson Amplitude (WAMP), and MYOPulse Percentage (MYOP) Rate.

1) RMS

The Root Mean Square (RMS) value represents the mean power of a signal over a window length of EMG samples. The mathematical equation to describe this feature is as follows [14]:

$$RMS = \sqrt{\frac{1}{N}\sum_{i=1}^{N} x_i^2}, \tag{1}$$

where x_i indicates the i^{th} EMG signal and N indicates the length of the EMG signal.

2) IEMG

The Integrated EMG (IEMG) value is an absolute summation of the EMG signal over a window length of EMG samples. The mathematical equation is described as follows [14]:

$$IEMG = \sum_{i=1}^{N} |x_i|\,. \tag{2}$$

3) VAR

The Variance of the EMG signal, EMG (VAR), is the average value of the power of the EMG signal. VAR is formulated as follows [14]:

$$VAR = \frac{1}{N-1}\sum_{i=1}^{N} \left|x_i^2\right|. \tag{3}$$

4) MAV

The Mean Absolute Value (MAV) is the average of the absolute value of the EMG signal for a window length N. The MAV is formulated as [14]:

$$MAV = \frac{1}{N}\sum_{i=1}^{N} |x_i|\,. \tag{4}$$

5) LOG

The Logarithm (LOG) parameter is a measure of the non-linear characteristic of the EMG signal. The LOG value is calculated based on the average of the logarithm of the EMG signal. The LOG value is defined as follows [14]:

$$LOG = \exp\left(\frac{1}{N}\sum_{i=1}^{N}\log(|x_i|)\right). \tag{5}$$

6) WL

The Waveform Length (WL) is used to measure the length of the signal between two consecutive samples x_{i+1} and x_i. WL is formulated as follows [14]:

$$WL = \sum_{i=1}^{N-1}|x_{i+1} - x_i|. \tag{6}$$

7) AAC

The Average Amplitude Change (AAC) is an the mean value of the waveform length within a window of length N. AAC is written as follows [14]:

$$ACC = \frac{1}{N}\sum_{i=1}^{N-1}|x_{i+1} - x_i|. \tag{7}$$

8) DASDV

The Difference Absolute Standard Deviation Value (DASDV) is calculated based on the standard deviation between x_{i+1} and x_i. DASDV is defined as follows [14]:

$$DASDV = \sqrt{\frac{1}{N-1}\sum_{i=1}^{N-1}(x_{i+1} - x_i)^2}. \tag{8}$$

9) ZC

The Zero Crossing (ZC) value is the number of time that the signal crosses a certain threshold value. ZC is calculated as [14]:

$$\begin{aligned} ZC &= \sum_{i=1}^{N-1}\left[f\left(x_i \cdot x_{i+1}\right) \cap |x_i - x_{i+1}|\right] \geq \text{threshold}, \\ f(x) &= \begin{cases} 1, & \text{if} \rightarrow x \geq \text{threshold}, \\ 0, & \text{otherwise}. \end{cases} \end{aligned} \tag{9}$$

10) SSC

The Sign Slope Change (SSC) is the number of times the slope of the signal changes its sign within a window of length N. It is formulated as follows [14]:

$$\begin{aligned} SSC &= \sum_{i=1}^{N-1}\left[f\left[(x_i - x_{i+1}) \cdot (x_i - x_{i+1})\right]\right], \\ f(x) &= \begin{cases} 1, & \text{if} \rightarrow x \geq \text{threshold}, \\ 0, & \text{otherwise}. \end{cases} \end{aligned} \tag{10}$$

11) WAMP

The Wilson Amplitude (WAMP) is the number of times that the absolute value of the difference between two consecutive samples (x_{i+1} and x_i) exceeds a threshold value. It is defined as follows [14]:

$$\begin{aligned} WAMP &= \sum_{i=1}^{N-1}\left[f\left(|x_i - x_{i+1}|\right)\right], \\ f(x) &= \begin{cases} 1, & \text{if} \rightarrow x \geq \text{threshold}, \\ 0, & \text{otherwise}. \end{cases} \end{aligned} \tag{11}$$

12) MYOP

The MyoPulse Percentage (MYOP) Rate is the average of the number of times that the EMG signal exceeds a predefined threshold. MYOP can be expressed as [15]:

$$\begin{aligned} MYOP &= \frac{1}{N}\sum_{i=1}^{N}\left[f\left(x_i\right)\right], \\ f(x) &= \begin{cases} 1, & \text{if} \rightarrow x \geq \text{threshold}, \\ 0, & \text{otherwise}. \end{cases} \end{aligned} \tag{12}$$

2.2. Infinite Impulse Response

It is obvious that the EMG signal has random and stochastic characteristics in nature [16]. Therefore, in order to smooth and reduce the noise contaminating this signal, filtering is required. Commonly, the filtering stage, as it has been performed in previous studies [12] and [17], is conducted by applying a digital Low-Pass Filtered (LPF) to process the EMG signal. In this study, an Infinite Impulse Response (IIR) LPF was designed and implemented. The LPF was constructed using a 2nd order Butterworth filter with cutoff frequencies set between 80 Hz and 100 Hz, respectively. The IIR filter was implemented using a cascade bi quad filter. This digital filter was then implemented by using the following difference equation [18]:

$$\begin{aligned} y[n] &= b_0x[n] + b_1x[n-1] + \cdots + b_Px[n-P] - \\ &+ a_1y[n-1] - a_2y[n-2] - \cdots - a_Qy[n-Q], \end{aligned} \tag{13}$$

where $x[n]$ indicates the nth input sample, $y[n]$ indicates the nth output sample, b_0, b_1, b_P, a_1, a_2, and a_Q are the filter coefficients, and $P = Q$ is the filter order.

3. Materials and Method

3.1. Participants

To implement the proposed method, four healthy male participants with no history of muscular disorder (age: 22.4 ± 3.2 years old, weight: 65.45 ± 5.67 kg) were recruited for this study after giving informed consent. Before the data collection process, the participants were recommended not to do any hard work especially anything that could potentially harm the elbow joint. The participants were instructed on how to perform the flexion and extension movements and were informed about any potential risk that could be involved in carrying out these motions.

Fig. 1: The Exoskeleton frame to synchronize the elbow-joint motion.

3.2. Equipment

A one-channel EMG system comprised of: a preamplifier, a band pass filter (with cut-off frequencies of 20 to 500 Hz, respectively), a summing amplifier, and an adjustable gain amplifier, was built. EMG signals were collected using three disposable surface (pregelled Ag/AgCl) bioelectrodes. Two bioelectrodes were positioned on the biceps muscle with the third one placed on the hand as a common ground electrode. The participants held an exoskeleton frame which was used to synchronize the elbow joint motion (see Fig. 1). The elbow joint angle of the exoskeleton was collected using a linear potentiometer which was located at the joint between the arm and forearm of the exoskeleton. A one kilogram (1 kg) load was placed on the forearm of the exoskeleton.

3.3. Data Collection

Before the data collection process, the participants were instructed to follow some specific steps. EMG signals were recorded while the subject's arm held the exoskeleton and moved it in flexion and extension motions within the range of 0 to 140°. As mentioned above, the exoskeleton was loaded with a 1 kg load (see Fig. 1). The motion periods were guided using a metronome program so that the flexion and extension movements could be regulated for 2 seconds, 4 seconds, 8 seconds and 10 seconds periods. EMG signals were recorded using a sampling frequency of 1000 Hz. For each period of motion, the participants performed flexion and extension motions for eight cycles (designated by C1, C2, C3, C4, C5, C6, C7, and C8) so that the total dataset comprised of 128 data points (4 participants $\times$ 4 periods $\times$ 8 cycles).

3.4. Data Processing

Figure 2 shows the processing of EMG signals to estimate the elbow joint angle. The collected EMG signals from biceps were processed to extract twelve Time-Domain (TD) features with a length of window of 200 milliseconds. The feature extraction process was conducted for each cycle of motion with the total of eight cycles. All of the extracted TD features such as: EMG_F (RMS, IEMG, VAR, MAV, LOG, WL, AAC, DASDV, ZC, SSC, WAMP, and MYOP) were calculated for each cycle and motion period. In order to obtain the estimated angle, the second order Butterworth low pass filter was then applied to smooth the features. As mentioned before, this IIR low pass filter was designed using the cut-off frequencies specified above to smooth out the EMG signals. The filtered feature Melbas then assumed as the estimated elbow joint angle. To evaluate the performance of the proposed method, the estimated elbow joint angle was analyzed using the Pearson's Correlation Coefficient (PCC) and Root Mean Squared Error (RMSE). The PCC was used to evaluate the relationship between the extracted TD features and the elbow joint angle. The RMSE value was used to evaluate the deviation between the estimated angle and the measured angle. The linearity of the estimated angle was also evaluated using linear regression parameters namely R^2, Slope and the Euclidian Distance.

3.5. Statistical Analysis

The statistical Analysis of Variance (ANOVA) was performed to observe if there was any statistical difference in performance and the regression parameters between the periods of motion (10 seconds, 8 seconds, 4 seconds,

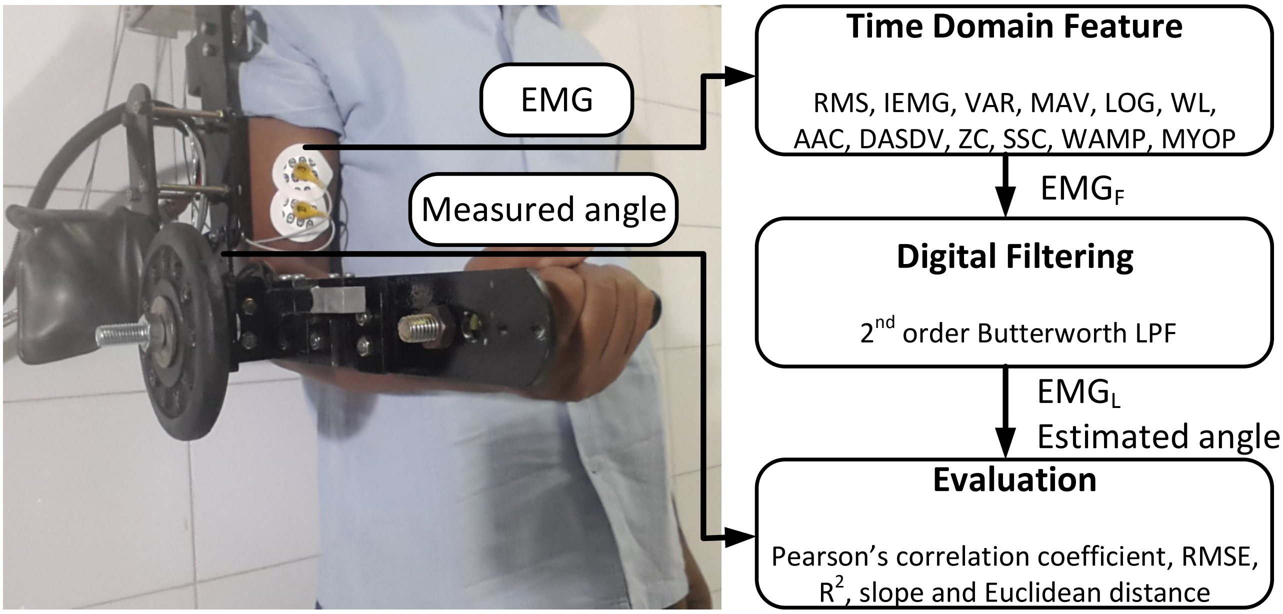

Fig. 2: The processing of EMG signas for flexion and extension movements to estimate the elbow joint angle. EMG signals were collected from biceps; time domain features were extracted and smoothed using a second order Butterworth low pass filter.

and 2 seconds). The significance test was established with confidence level of 95 % (alpha = 0.05).

4. Results and Discussion

The recorded EMG signals and the measured angles acquired from four participants were processed offline for feature extraction and evaluation. A predefined threshold was required for ZC, SSC, WAMP, and MYOP features. The cut-off frequency of the LPF was also essential which determined the smoothness of the estimated angle. In this work, the threshold and cut-off frequencies were chosen such that elbow joint angle estimation could be made at the maximum performance. The detailed results of this study are explained and discussed in the following subsection.

4.1. Accuracy of the Elbow Joint Angle Estimation

In this work, a relationship between the estimated angle and the measured angle was indicated by the PCC. A coefficient score approaching 1 indicates that there is a strong relationship and a score approaching 0 shows that there is a weak relationship. In the motion period of 10 seconds Fig. 3(a) and Fig. 3(b), the results show that the estimated angles based on the MYOP feature have the highest correlation coefficient (0.97 ± 0.02) (Mean±SD) and the lowest RMSE ($11.37 \pm 3.04°$) (Mean±SD) value. In the motion period of 8 seconds, as shown in Fig. 3(c) and Fig. 3(d), the estimated angle based on the MYOP feature shows the highest correlation coefficient (0.97 ± 0.01) and the lowest RMSE ($11.25 \pm 2.44°$) value. Figure 3(e) and Fig. 3(f) show that the estimated angle from the MYOP feature has the highest accuracy (correlation coefficient $= 0.91 \pm 0.04$ and RMSE $= 17.58 \pm 3.08°$). The highest accuracies of the estimated angle are also found from the estimated angle based on the MYOP feature in the motion period of 2 seconds (0.88 ± 0.05 and $20.13 \pm 2.69°$ for correlation coefficient and RMSE, respectively). Over all periods of motion, there is a minimum of RMSE of 6.07° and a maximum correlation of 0.99 that occurred in the 10 second period of motion. Among the other features, the correlation coefficient of the estimated angle from Zero Crossing (ZC) feature showed the widest variance (Fig. 3(a), Fig. 3(b), Fig. 3(c), Fig. 3(d), Fig. 3(e) and Fig. 3(f)). The estimated angle based on the VAR feature showed wider variance of RMSE compared to the other features. The ANOVA tests showed that there was a significant difference (p-value < 0.05) in accuracy between groups of periods (10 seconds, 8 seconds, 4 seconds and 2 seconds) for all features except for the MYOP feature. In the period of motion of 8 seconds and 10 seconds, the MYOP feature showed that there was no significant difference in the RMSE value (p-value > 0.05). This indicates that the estimated angle using the MYOP feature is more consistent and produces higher accuracy to estimate the elbow joint angle for different motion periods compared to the other features.

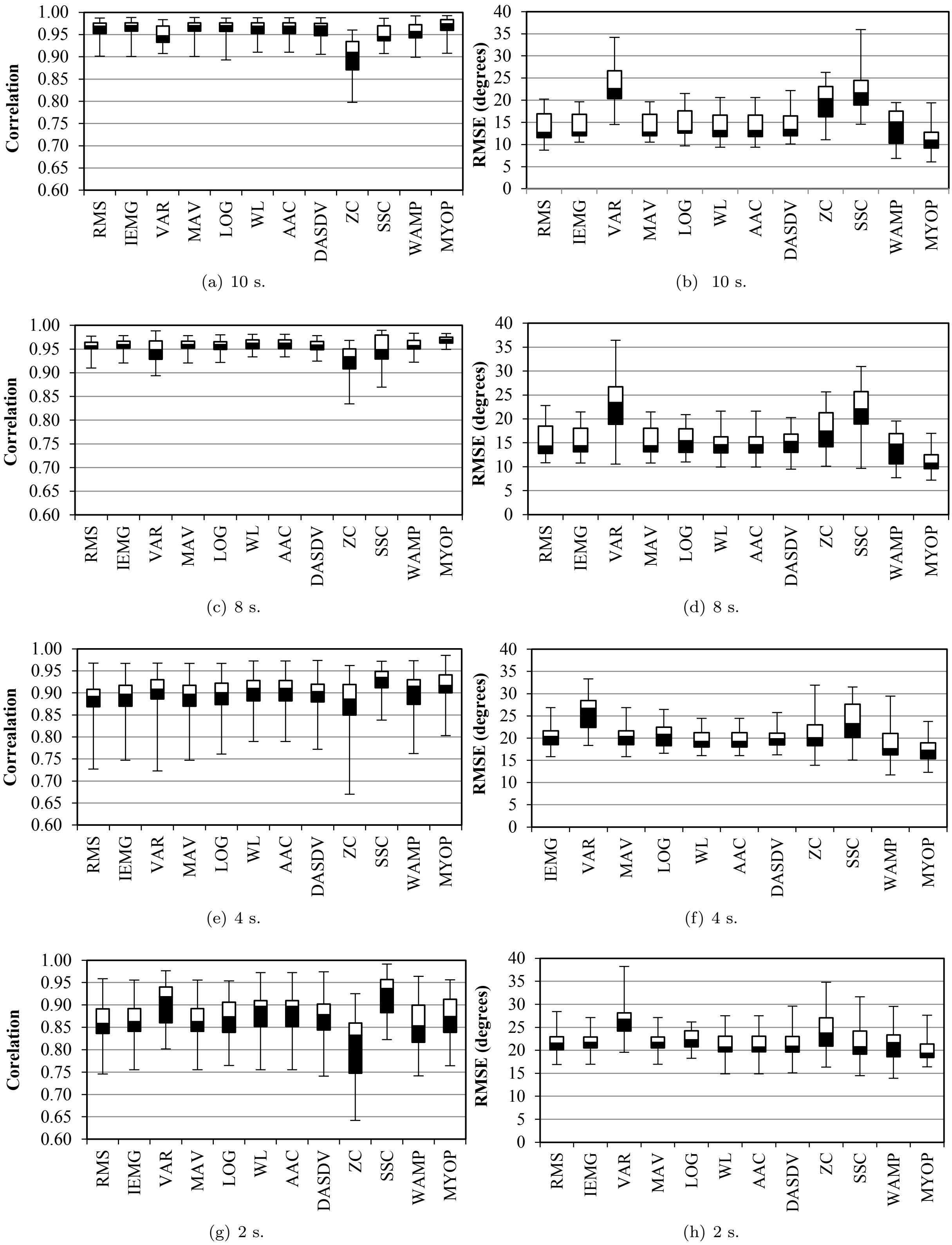

Fig. 3: The effect of TD features on the accuracy of the elbow joint angle estimation. The box plot of Pearson's Correlation Coefficient were calculated for the following periods of motion: (a) 10 s, (c) 8 s, (e) 4 s and (g) 2 s. The box plot of the RMSE value for periods of motion: (b) 10 s, (d) 8 s, (f) 4 s and (h) 2 s.

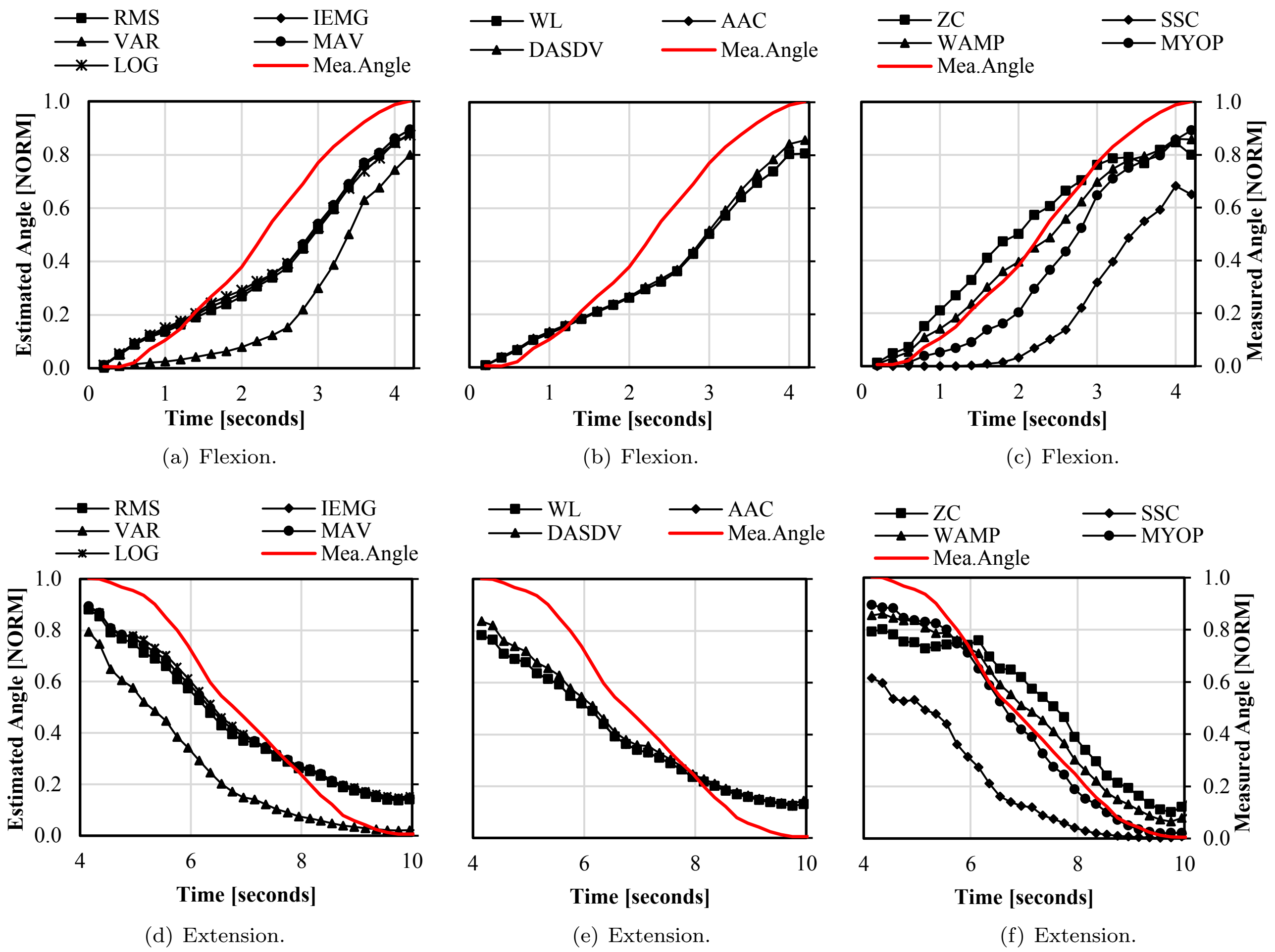

(a) Flexion. (b) Flexion. (c) Flexion.

(d) Extension. (e) Extension. (f) Extension.

Fig. 4: Typical time response for the normalized estimated angle for a motion period of 10 seconds. The estimated angle based on RMS, IEMG, VAR, MAV, and LOG features for (a) flexion and (d) extension motions. The estimated angle from WL, AAC, and DASDV features for (b) flexion and (e) extension motions. The estimated angle from ZC, SSC, WAMP and MYOP features for (c) flexion and (f) extension motions.

The results of our proposed method are comparable with those presented in several previous studies [3] and [19]. Pau et al. developed a model to estimate the elbow joint angle using the Hill-based method and a genetic algorithm in two muscle groups (biceps and triceps) [3]. In their study, they achieved an RMSE value of $18.6 \pm 6.5°$ for five continuous cycles.

Tang et al. studied the elbow joint angle estimation problem using artificial neural networks as a classifier. In their research, they utilized four muscle groups (biceps brachii, brachioradialis, triceps brachii and anconeus). The RMSE values of their model were 10.7°, 9.67°, 12.42° for motion period of 2 seconds, 4 seconds, and 8 seconds, respectively [19].

4.2. Response of Estimated Angle to Time

Figure 4(a), Fig. 4(b), Fig. 4(c), Fig. 4(d), Fig. 4(e) and Fig. 4(f) show a typical response of the estimated angle to time for a motion period of 10 seconds (red line indicate the measured angle). Ideally, the estimated angle should be comparable to the measured angle. To test this proximity, the Euclidean Distance (ED) was calculated to present the closeness between the pattern of the estimated angle and the measured angle as shown in Eq. (14):

$$ED = \sqrt{\sum_{i=1}^{N} (EMG_L - Angle_i)^2}, \qquad (14)$$

Tab. 1: The Euclidean Distance between elbow joint angle and features for flexion and extension motions (period of motion: 10 seconds, 8 seconds, 4 seconds, and 2 seconds). The bold text indicates the lowest value of the Euclidean Distance.

Features	**Flexion motion (NORM)**				**Extension motion (NORM)**			
	$T = 10{\sim}$s	$T = 8{\sim}$s	$T = 4{\sim}$s	$T = 2{\sim}$s	$T = 10{\sim}$s	$T = 8{\sim}$s	$T = 6{\sim}$s	$T = 2{\sim}$s
RMS	0.671	0.921	0.615	0.729	0.741	0.606	0.52	0.547
IEMG	0.625	0.898	0.61	0.761	0.682	0.597	0.519	0.563
VAR	1.34	1.598	1.023	1.088	1.493	1.202	0.686	0.742
MAV	0.625	0.898	0.61	0.761	0.682	0.597	0.519	0.563
LOG	0.654	0.884	0.622	0.786	0.66	0.602	0.545	0.587
WL	0.76	1.091	0.645	0.715	0.952	0.699	0.548	0.595
AAC	0.76	1.091	0.645	0.715	0.952	0.699	0.548	0.595
DASDV	0.696	1.039	0.661	0.718	0.827	0.632	0.551	0.575
ZC	0.445	**0.313**	0.289	0.244	0.805	0.766	0.602	0.642
SSC	1.449	1.547	1.08	0.974	1.709	1.003	0.763	0.618
WAMP	**0.312**	0.325	**0.242**	**0.341**	0.452	0.445	0.549	0.565
MYOP	0.581	0.624	0.532	0.678	**0.329**	**0.191**	**0.43**	**0.496**

Tab. 2: The Linear Regression R^2 values between the estimated and measured angles. The R^2 values were calculated for all periods of motion (10 second, 8 seconds, 4 seconds, and 2 seconds) for the flexion and extension movements.

Features	**Flexion**				**Extension**			
	$T = 10{\sim}$s	$T = 8{\sim}$s	$T = 4{\sim}$s	$T = 2{\sim}$s	$T = 10{\sim}$s	$T = 8{\sim}$s	$T = 6{\sim}$s	$T = 2{\sim}$s
RMS	0.952	0.949	0.965	0.969	0.974	0.995	0.993	0.981
IEMG	0.956	0.947	0.967	0.968	0.981	0.993	0.995	0.985
VAR	0.824	0.812	0.86	0.813	0.916	0.949	0.993	0.997
MAV	0.956	0.947	0.967	0.968	0.981	0.993	0.995	0.985
LOG	0.957	0.942	0.973	0.967	0.988	0.99	0.994	0.988
WL	0.962	0.939	0.971	0.978	0.977	0.993	0.995	0.988
AAC	0.962	0.939	0.971	0.978	0.977	0.993	0.995	0.988
DASDV	0.955	0.943	0.966	0.974	0.974	0.996	0.993	0.986
ZC	0.946	0.99	0.977	0.964	0.856	0.889	0.914	0.91
SSC	0.852	0.831	0.847	0.863	0.968	0.964	0.987	0.993
WAMP	0.995	0.998	0.995	0.993	0.976	0.996	0.942	0.93
8 MYOP	0.979	0.987	0.997	0.993	0.989	0.991	0.983	0.971

Tab. 3: The Linear Regression Slope values between the estimated and the measured angle. The slopes were calculated for all periods of motion (10 seconds, 8 seconds, 4 seconds, and 2 seconds) for the flexion and extension movements.

Features	**Flexion**				**Extension**			
	$T = 10{\sim}$s	$T = 8{\sim}$s	$T = 4{\sim}$s	$T = 2{\sim}$s	$T = 10{\sim}$s	$T = 8{\sim}$s	$T = 6{\sim}$s	$T = 2{\sim}$s
RMS	0.752	0.693	0.608	0.466	−0.735	−0.619	−0.535	−0.434
IEMG	0.761	0.703	0.609	0.446	−0.752	−0.622	−0.534	−0.418
VAR	0.68	0.569	0.499	0.299	−0.806	−0.51	−0.533	−0.394
MAV	0.761	0.703	0.609	0.446	−0.752	−0.622	−0.534	−0.418
LOG	0.733	0.712	0.597	0.432	−0.757	−0.616	−0.507	−0.399
WL	0.707	0.639	0.593	0.484	−0.652	−0.585	−0.505	−0.394
AAC	0.707	0.639	0.593	0.484	−0.652	−0.585	−0.505	−0.394
DASDV	0.743	0.656	0.583	0.483	−0.701	−0.613	−0.502	−0.406
ZC	0.766	0.852	0.804	0.825	−0.454	−0.811	−0.548	−0.452
SSC	0.637	0.624	0.488	0.426	−0.726	−0.627	−0.514	−0.47
WAMP	0.822	0.889	0.831	0.726	−0.702	−0.88	−0.666	−0.511
MYOP	0.892	0.851	0.727	0.554	−0.917	−0.909	−0.621	−0.497

where N indicates the number of samples, $Angle_i$ stands for the-ith measured angle and the EMG_L shows the filtered features (estimated angle). In general, a small value of ED indicates a close relationship between the estimated angle and the measured angle. ED was measured for all periods of motion (10 seconds, 8 seconds, 4 seconds and 2 seconds) and for all of the TD features.

Table 1 shows the summary of the ED values for all motion periods and features. The estimated angle based on the WAMP feature tended to show smaller ED values in the elbow flexion trajectory (for all periods of motion) compared to those based on the other features. For the elbow extension trajectory, the estimated angles based on the MYOP feature showed the lowest value (0.329, 0.191, 0.430, and 0.496 for motion period of 10 seconds, 8 seconds, 4 seconds and 2 seconds, respectively). The estimated angle based on the VAR feature tended to have higher Euclidean Distance values compared to other features for all periods of motion.

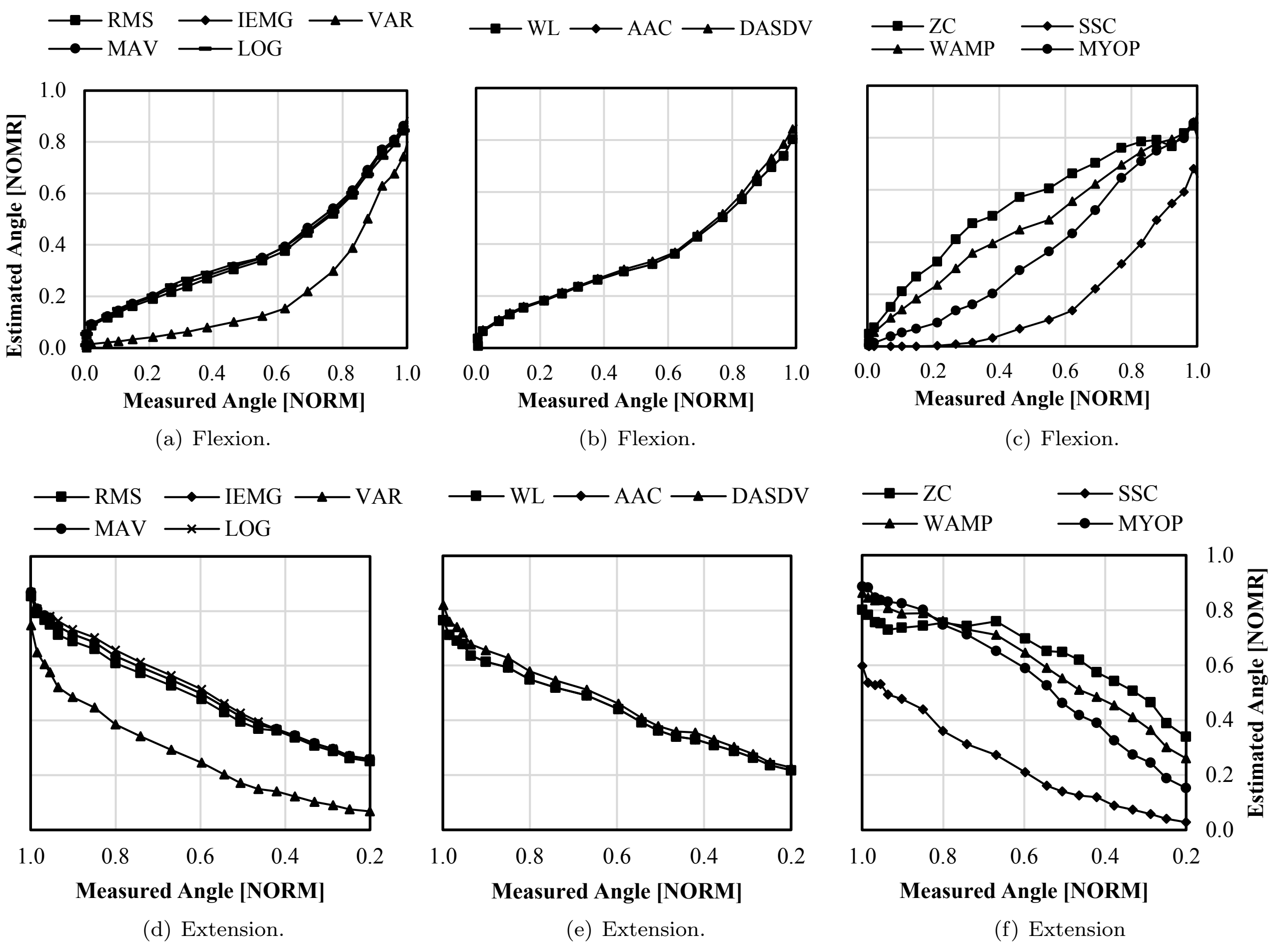

Fig. 5: The relationship between the normalized measured angle to the normalized EMG features during flexion (a), (b), and (c), and extension (d), (e), and (f) for period of motion = 10 seconds.

4.3. The Effects of the Elbow Joint Angle on EMG Signal Features

Figure 5 shows a typical relationship between the estimated and measured angles for both flexion and extension movements (period of motion = 10 seconds). The R^2 and Slope values were calculated to evaluate the linear regression between the estimated and measured angle as shown in Tab. 2 and Tab. 3. Table 2 shows that the R^2 of the estimated angle from the MYOP and WAMP features are higher and more consistent for all periods of motion (ranged between 0.938 and 0.998) compared to those calculated from other features. This means that the estimated angles were fitted closely to the measured angles.

The R^2 values of the model developed by Tang et al. were 0.83, 0.87 and 0.79 for the periods of motion 2 seconds, 4 seconds and 8 seconds, respectively [19]. Table 3 shows several of the Slope values for various EMG features. In the flexion trajectory, the estimated angle based on the WAMP and MYOP features showed the best Slope value (ranged from 0.727 to 0.889). In the extension trajectory, the estimated angle based on the MYOP feature had the best Slope value (ranged from −0.917 to −0.909 for periods of motion 10 seconds and 8 seconds, respectively).These values indicated that the estimated angle was almost linearly related to the measured angle. The negative value indicated a negative response between the measured angle and the estimated angle. From the ANOVA test, unfortunately, we found that there was a significant difference (p-value < 0.05) between the Slopes during extension and flexion movements. The Slope values decreased for the periods of motions from 10 seconds, 8 seconds, 4 seconds and 2 seconds, respectively. Ideally, the slope of the features should be constant so that the model can be used for any periods of motion. In the future, a model that can compensate the decrement of the slope is needed.

5. Conclusion

This study presents an investigation of TD features to estimate the elbow joint angle using EMG features based on a non-pattern recognition method. Some parameters such as the: Pearson's Correlation Coefficient, Root Mean Squared Error, Euclidean Distance, R^2, Linear Regression Slope were evaluated to obtain the best EMG features in estimating the elbow joint angle. The EMG signals for this study were collected from biceps alone enabled us to estimate the elbow joint angle. Our findings show that for a 10 second long recording period, the MyoPulse Percentage (MYOP) Rate produced the best accuracy: with PCC of 0.97 ± 0.02 (Mean±SD) and RMSE of $11.37 \pm 3.04°$ (Mean±SD), respectively. The MYOP feature also showed the highest R^2 and Slope value 0.986 ± 0.0083 (Mean±SD) and 0.746 ± 0.17 (Mean±SD), respectively for flexion and extension motions during all recorded periods.

References

[1] OSKOEI, M. A. and H. HU. Myoelectric control systems-A survey. *Biomedical Signal Processing and Control*. 2007, vol. 2, iss. 4, pp. 275–294. ISSN 1746-8094. DOI: 10.1016/j.bspc.2007.07.009.

[2] TRIWIYANTO, O. WAHYUNGGORO, H. A. NUGROHO and HERIANTO. Quantitative relationship between feature extraction of sEMG and upper limb elbow joint angle. In: *International Seminar on Application for Technology of Information and Communication (ISemantic)*. Semarang: IEEE, 2016, pp. 44–50. ISBN 978-1-5090-2326-4. DOI: 10.1109/ISEMANTIC.2016.7873808.

[3] PAU, J. W. L., S. S. Q. XIE and A. J. PULLAN. Neuromuscular Interfacing: Establishing an EMG-Driven Model for the Human Elbow Joint. *IEEE Transactions on Biomedical Engineering*. 2012, vol. 59, iss. 9, pp. 2586–2593. ISSN 1558-2531. DOI: 10.1109/TBME.2012.2206389.

[4] TANG, Z., H. YU and S. CANG. Impact of Load Variation on Joint Angle Estimation From Surface EMG Signals. *IEEE Transactions on Neural Systems and Rehabilitation Engineering*. 2016, vol. 24, iss. 12, pp. 1342–1350. ISSN 1558-0210. DOI: 10.1109/TNSRE.2015.2502663.

[5] BENITEZ, L. M. V., M. TABIE, N. WILL, S. SCHMIDT, M. JORDAN and E. A. KIRCHNER. Exoskeleton Technology in Rehabilitation: Towards an EMG-Based Orthosis System for Upper Limb Neuromotor Rehabilitation. *Journal of Robotics*. 2013, vol. 2013, iss. 1, pp. 1–13. ISSN 1687-9600. DOI: 10.1155/2013/610589.

[6] JANG, G., J. KIM, Y. CHOI and J. YIM. Human shoulder motion extraction using EMG signals. *International Journal of Precision Engineering and Manufacturing*. 2014, vol. 15, iss. 10, pp. 2185–2192. ISSN 2005-4602. DOI: 10.1007/s12541-014-0580-x.

[7] LI, Q., Y. SONG, Z. HOU and B. ZHU. sEMG Based Joint Angle Estimation of Lower Limbs Using LS-SVM. In: *20th International Conference on Neural Information Processing (ICONIP)*. Daegu: Springer, 2013, pp. 292–300. ISBN 978-364242053-5. DOI: 10.1007/978-3-642-42054-2_37.

[8] LOCONSOLE, C., S. DETTORI, A. FRISOLI, C. A. AVIZZANO and M. BERGAMASCO. An EMG-based approach for on-line predicted torque control in robotic-assisted rehabilitation. In: *2014 IEEE Haptics Symposium (HAPTICS)*. Houston: IEEE, 2014, pp. 181–186. ISBN 978-1-4799-3131-6. DOI: 10.1109/HAPTICS.2014.6775452.

[9] REZA, S. M. T., N. AHMAD, I. A. CHOUDHURY and R. A. R. GHAZILLA. A Fuzzy Controller for Lower Limb Exoskeletons during Sit-to-Stand and Stand-to-Sit Movement Using Wearable Sensors. *Sensors*. 2014, vol. 14, iss. 3, pp. 4342–4363. ISSN 1424-8220. DOI: 10.3390/s140304342.

[10] TSAI, A.-C., T.-H. HSIEH, J.-J. LUH and T.-T. LIN. A comparison of upper-limb motion pattern recognition using EMG signals during dynamic and isometric muscle contractions. *Biomedical Signal Processing and Control*. 2014, vol. 11, iss. 1, pp. 17–26. ISSN 1746-8094. DOI: 10.1016/j.bspc.2014.02.005.

[11] LENZI, T., S. M. M. D. ROSSI, N. VITIELLO and M. C. CARROZZA. Intention-Based EMG Control for Powered Exoskeletons. *IEEE Transactions on Biomedical Engineering*. 2012, vol. 59, iss. 8, pp. 2180–2190. ISSN 1558-2531. DOI: 10.1109/TBME.2012.2198821.

[12] LEE, S., H. KIM, H. JEONG and J. KIM. Analysis of musculoskeletal system of human during lifting task with arm using electromyography. *International Journal of Precision Engineering and Manufacturing*. 2015, vol. 16, iss. 2, pp. 393–398. ISSN 2005-4602. DOI: 10.1007/s12541-015-0052-y.

[13] PHINYOMARK, A., P. PHUKPATTARANONT and C. LIMSAKUL. Feature reduction and selection for EMG signal classification. *Expert Systems with Applications*. 2012, vol. 39, iss. 8, pp. 7420–7431. ISSN 0957-4174. DOI: 10.1016/j.eswa.2012.01.102.

[14] CHOWDHURY, R. H., M. B. I. REAZ, M. A. B. M. ALI, A. A. A. BAKAR, K. CHELLAPPAN and T. G. CHANG. Surface Electromyography Signal Processing and Classification Techniques. *Sensors*. 2013, vol. 13, iss. 9, pp. 12431–12466. ISSN 1424-8220. DOI: 10.3390/s130912431.

[15] FOUGNER, A. L. *Proportional MyoelectricControl of a Multifunction Upper-limb Prosthesis*. Trondheim, 2007. Thesis. Norwegian University of Science and Technology. Supervisor Tor Engebret Onshus.

[16] LUCA, C. J. D. Surface Electromyography: Detection and Recording. In: *DelSys* [online]. 2002. Available at: http://www.ti.com/lit/an/slva372c/slva372c.pdf.

[17] JANG, G., J. KIM, Y. CHOI and J. YIM. Human shoulder motion extraction using EMG signals. *International Journal of Precision Engineering and Manufacturing*. 2014, vol. 15, iss. 10, pp. 2185–2192. ISSN 2234-7593. DOI: 10.1007/s12541-014-0580-x.

[18] TAN, L. *Digital Signal Processing Fundamentals and Applications*. 1st ed. San Diego: Elsevier, 2008. ISBN 978-0-0805-5057-2.

[19] TANG, Z., K. ZHANG, S. SUN, Z. GAO, L. ZHANG and Z. YANG. An upper-limb power-assist exoskeleton using proportional myoelectric control. *Sensors*. 2014, vol. 14, iss. 10, pp. 6677–6694. ISSN 1424-8220. DOI: 10.3390/s140406677.

About Authors

TRIWIYANTO was born in Surabaya, Indonesia. He received his M.Sc. degree in Electronic Engineering in Institute of Technology Sepuluh Nopember in 2004, Surabaya, Indonesia. He is currently a Ph.D. candidate in Electrical Engineering at Gadjah Mada University, Yogyakarta, Indonesia. His research interests include biomedical signal analysis, embedded system, electronic instrumentation, assistive and rehabilitation devices.

Oyas WAHYUNGGORO was born in Jogjakarta, Indonesia. He received his Ph.D. degree in Electrical and Electronic Engineering from the Universiti Teknologi Petronas, Malaysia in 2011. His research interests include biomedical signal processing, intelligent system, and control system.

Hanung Adi NUGROHO was born in Jogjakarta, Indonesia. He received his Ph.D. degree in Electrical and Electronic Engineering from the Universiti Teknologi Petronas, Malaysia in 2012. His research interests include biomedical signal processing and image processing.

HERIANTO was born in Jogjakarta, Indonesia. He received his D.Eng. degree in the Department of Mechanical and Control Engineering, Tokyo Institute of Technology, Japan, in 2009. His research interests include robotics and manufacture. His current research is product design and development especially in rehabilitation robot.